arXiv:1703.08938v2 [physics.optics] 12 Apr 2017

Edge states in dynamical superlattices

Yiqi Zhang[1],* Yaroslav V. Kartashov[3,4,5], Feng Li[1], Zhaoyang Zhang[1,2], Yanpeng Zhang[1],† Milivoj R. Belić[6], and Min Xiao[7,8]

[1]*Key Laboratory for Physical Electronics and Devices of the Ministry of Education & Shaanxi Key Lab of Information Photonic Technique, Xi'an Jiaotong University, Xi'an 710049, China*

[2]*Department of Applied Physics, School of Science, Xi'an Jiaotong University, Xi'an 710049, China*

[3]*ICFO-Institut de Ciencies Fotoniques, The Barcelona Institute of Science and Technology, 08860 Castelldefels (Barcelona), Spain*

[4]*Institute of Spectroscopy, Russian Academy of Sciences, Troitsk, Moscow Region 142190, Russia*

[5]*Department of Physics, University of Bath, Bath BA2 7AY, United Kingdom*

[6]*Science Program, Texas A&M University at Qatar, P.O. Box 23874 Doha, Qatar*

[7]*Department of Physics, University of Arkansas, Fayetteville, Arkansas, 72701, USA*

[8]*National Laboratory of Solid State Microstructures and School of Physics, Nanjing University, Nanjing 210093, China*

(Dated: April 13, 2017)

We address edge states and rich localization regimes available in the one-dimensional (1D) dynamically modulated superlattices, both theoretically and numerically. In contrast to conventional lattices with straight waveguides, the quasi-energy band of infinite modulated superlattice is periodic not only in the transverse Bloch momentum, but it also changes periodically with increase of the coupling strength between waveguides. Due to collapse of quasi-energy bands dynamical superlattices admit known dynamical localization effect. If, however, such a lattice is truncated, periodic longitudinal modulation leads to appearance of specific edge states that exist within certain periodically spaced intervals of coupling constants. We discuss unusual transport properties of such truncated superlattices and illustrate different excitation regimes and enhanced robustness of edge states in them, that is associated with topology of the quasi-energy band.

PACS numbers: 03.65.Vf, 42.25.Gy, 78.67.–n

* zhangyiqi@mail.xjtu.edu.cn

† ypzhang@mail.xjtu.edu.cn

I. INTRODUCTION

Periodically modulated lattice systems attract considerable attention in diverse areas of physics, including condensed matter physics [1–9] and photonics [10–19]. One of the main reasons behing interest to such systems is that due to variation of parameters of the system along the evolution coordinate (time in condensed matter physis or propagation distance in photonics) not only rich variety of resonant dynamical effects associated with specific deformations of quasi-energy bands appears (for an overview of such dynamical effects see [20, 21]), but one may also encounter the effects of purely topological origin. One of the manifestations of such effects is the appearance of topologically protected edge states that are typically unidirectional (in the 2D systems) and that demonstrate immunity to backscattering on disorder and other structural lattice defects due to topological protection. In modulated periodic photonic systems, frequently called Floquet insulators [3, 15, 22, 23], longitudinal variations of underlying potential were shown to lead to appearance of the effective external time-dependent "magnetic fields" that qualitatively change the behaviour of the system and allow to design a new class of devices employing topologically protected transport, including photonic interconnects, delay lines, isolators, couplers, and other structures [23]. Periodically modulated photonic lattices were employed for realization of discrete quantum walks [24, 25], and allowed observation of Floquet topological transitions with matter waves [26, 27].

Previous investigations of modulated lattices were mainly focused on the 2D and 3D geometries, and less attention was paid to the 1D settings. Moreover, upon consideration of bulk and surface effects in the modulated photonic 1D systems only simplest lattices were utilized with identical coupling strength between all channels and with identical (usually sinusoidal) laws of their longitudinal variation [28–34]. Only recently dynamical *superlattices* with specially designed periodically varying separation between channels belonging to two different sublattices were introduced that allowed observation of intriguing new resonant phenomena, such as light rectification [35–37]. Previously only bulk modulated superlattices were considered and no surface effects in such structures were addressed. Therefore, main aim of this work is the exploration of new phenomena stemming from the interplay between superlattice truncation and its longitudinal modulation. We aim to show that dynamically modulated *truncated* superlattices exhibit topological transition manifested in qualiative modification of the quasi-energy spectrum upon variation of the coupling strength between waveguides forming the lattice. Namely, within proper intervals of coupling strength the isolated eigenvalues appear that are associated with nonresonant (i.e. existing within continuous intervals of coupling strengths) edge states. Interestingly, such edge states persist even when conditions for collapse of bulk quasi-energy band are met. We discuss specific propagation dynamics in the regime, where edge states exist. We believe that these findings substantially enrich the approaches for control of propagation paths of light beams in periodic media.

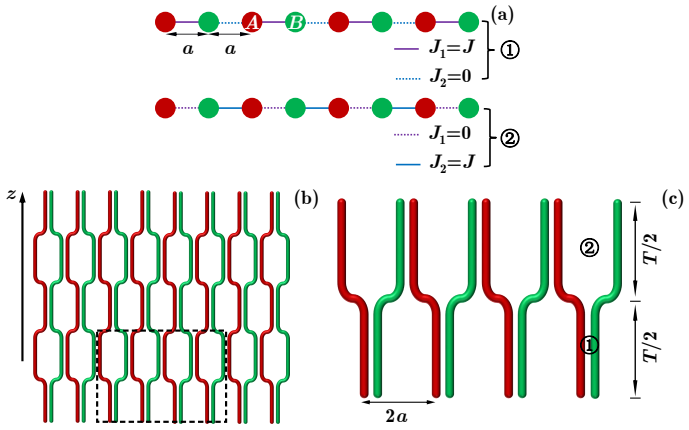

FIG. 1. (a) Shematic illustration showing coupling constants on two half-periods of superlattice composed from sublattices A and B. Coupling only occurs between sites connected by solid lines and is absent between sites connected by dashed lines. (b) Refractive index distribution in photonic lattice that reproduces coupling scheme illustrated in panel (a). (c) Magnification of the region marked by a dashed box in (b) that shows one longitudinal period of the structure.

As an example of the dynamical superlattice we consider discrete structure depicted in Fig. 1, which is somewhat similar to the Su-Schrieffer-Heeger lattice [38]. The superlattice is composed of two sublattices, denoted as A and B (red and green channels in Fig. 1). The single-mode waveguides in individual sublattices are curved such that coupling strength between nearest neighbours belonging to different sublattices changes with propagation distance in a step-like fashion, as shematically shown in Fig. 1(a) [since there are two sublattices, one can introduce two coupling strengths $J_1(z)$ and $J_2(z)$ describing coupling between waveguides with equal (n, n) or with different $(n, n+1)$ indices

from two sublattices]. We assume that the coupling strength increases to maximal value J when two waveguides are close and drops down nearly to zero when they are well separated, due to exponential decrease of the overlap integrals between modal fields with increase of the distance between waveguides. The longitudinal period of the structure is given by T, while transverse period is given by $2a$. In Fig. 1(c) we display one longitudinal period of the structure indicated by a dashed box in Fig. 1(b). Coupling constants on two different segments of the lattice are indicated in Fig. 1(a). Such a lattice can be easily fabricated with femtosecond-laser writing technique [15, 36, 39–42].

II. THEORETICAL MODEL AND BAND STRUCTURE

We describe propagation of light in the infinite superlattice depicted in Fig. 1 using discrete model [43, 44]

$$\begin{aligned} i\frac{dA_n}{dz} &= J_1(z)B_n + J_2(z)B_{n-1}, \\ i\frac{dB_n}{dz} &= J_1(z)A_n + J_2(z)A_{n+1}, \end{aligned} \tag{1}$$

where coupling constants $J_{1,2}(z)$ are step-like periodic functions of the propagation distance z, while A_n, B_n stand for the field amplitudes on sites of sublattices A and B. According to the Floquet theory, the evolution of excitations in longitudinally modulated lattice governed by the Hamiltonian $H(\mathbf{k},t) = H(\mathbf{k},t+T)$ (here T is the period of longitudinal modulation and $\mathbf{k}$ is the transverse Bloch momentum), can be described by the Floquet evolution operator $U(t) = \mathcal{T}\exp[-i\int_0^t H(\mathbf{k},t')dt']$, where $\mathcal{T}$ is the time-ordering operator. Defining evolution operator $U(T)$ for one longitudinal period of the structure [i.e. $|\phi(\mathbf{k},T)\rangle = U(T)|\phi(\mathbf{k},0)\rangle$, where $|\phi(\mathbf{k},t)\rangle$ is the Floquet eigenstate of the system] and using adiabatic approximation, one can introduce effective Hamiltonian H_{eff} of the modulated lattice in accordance with definition $U(T) = \exp(-iH_{\text{eff}}T)$. In contrast to instantaneous Hamiltonian $H(\mathbf{k},t)$, the effective Hamiltonian H_{eff} is z-independent, and it offers "stroboscopic" description of the propagation dynamics over complete longitudinal period. The spectrum of the system can be described by quasi-energies ϵ — eigenvalues of the effective Hamiltonian [45, 46] — that can be obtained from the expression $U(T)|\phi\rangle = \exp(-i\epsilon T)|\phi\rangle$. Using this approach in the case of infinite discrete lattice we search for solutions of Eq. (1) in the form of periodic Bloch waves $A_n = A\exp(ikx_n)$ and $B_n = B\exp(ikx_n + ika)$, where $x_n = 2na$ is the discrete transverse coordinate, and $k \in [-\pi/2a, \pi/2a]$ is the Bloch momentum in the first Brillouin zone. Substituting these expressions into Eq. (1), one obtains

$$\begin{aligned} i\frac{dA}{dz} &= [J_1(z)\exp(iak_x) + J_2(z)\exp(-iak_x)]B, \\ i\frac{dB}{dz} &= [J_1(z)\exp(-iak_x) + J_2(z)\exp(iak_x)]A. \end{aligned} \tag{2}$$

Thus, Floquet evolution operator over one period can be represented as[2, 4, 23]

$$\begin{aligned} U(T) &= \exp(-iH_2T/2)\exp(-iH_1T/2) \\ &= \cos(ak)\exp(-iak)\times \\ &\begin{bmatrix} \cos(JT) + i\tan(ak) & i\exp(iak)\sin(JT) \\ i\exp(iak)\sin(JT) & \exp(2iak)[\cos(JT) - i\tan(ak)] \end{bmatrix}, \end{aligned} \tag{3}$$

where Hamiltonians on the first and second half-periods are given by

$$H_1 = \begin{bmatrix} 0 & J\exp(iak) \\ J\exp(-iak) & 0 \end{bmatrix},$$
$$H_2 = \begin{bmatrix} 0 & J\exp(-iak) \\ J\exp(iak) & 0 \end{bmatrix}.$$

One can see from Eq. (3) that Floquet evolution operator is a periodic function of transverse momentum k with a period π/a and of the coupling strength J with a period $2\pi/T$. Similarly, by introducing the effective Hamiltonian through $U = \exp(-iH_{\text{eff}}T)$ and calculating its eigenvalues (quasi-energies ϵ), one obtains that the latter are also periodic functions of k and J. In Fig. 2, we depict the dependence $\epsilon(k,J)$. Quasi-energy band is symmetric with respect to the plane $\epsilon = 0$ (it is periodic also in the vertical direction with a period $2\pi/T$ because eigenvalues of periodic system are defined modulo $2\pi/T$). The maxima of quasi-energies within vertical interval shown in Fig. 2 are located at $k = n\pi/a$ and $J = (2l+1)\pi/T$, where n is an integer and l is a non-negative integer. To highlight the

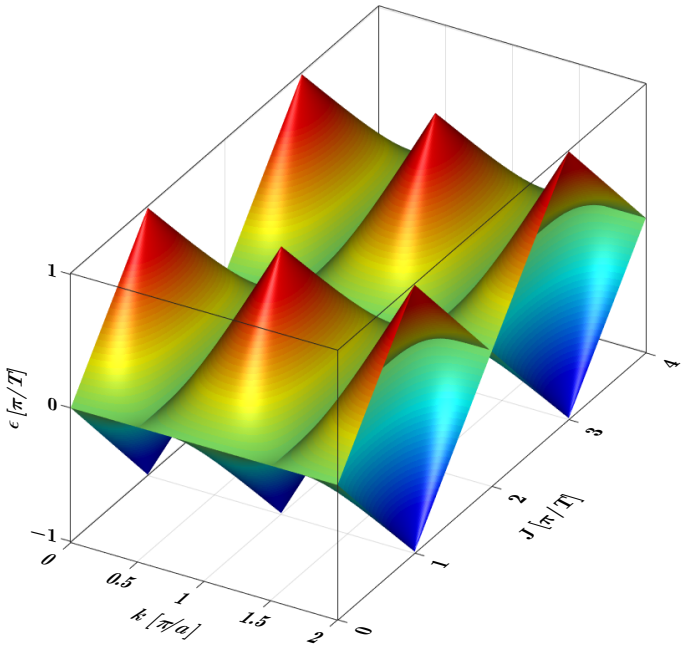

FIG. 2. Quasi-energy as a function of Bloch momentum k and coupling constant J.

details of this dependence we show quasi-energies in Figs. 3(a) and 3(b) for certain fixed values of coupling strength J and Bloch momentum k, respectively. Importantly, it follows from Fig. 3(a) that the quasi-energy band is dispersive at $J < \pi/T$ (see red curves), so for this coupling strength any localized wavepacket launched into system will diffract. When J increases up to π/T the dependence $\epsilon(k)$ becomes linear [47] (see black lines). This means that effective dispersion coefficient vanishes and excitations in such a lattice will propagate without diffraction, but with nonzero transverse velocity — this is the rectification regime. Further increase of the coupling strength makes quasi-energy band dispersive again. Finally, quasi-energy band collapses to a line at $J = 2\pi/T$ (see the blue line). In this regime of dynamical localization the shape of any wavepacket launched into system will be exactly reproduced after one longitudinal period. Very similar transformations can be observed for different Bloch momenta, when quasi-energy is plotted as a function of coupling constant J, as shown in Fig. 3(b).

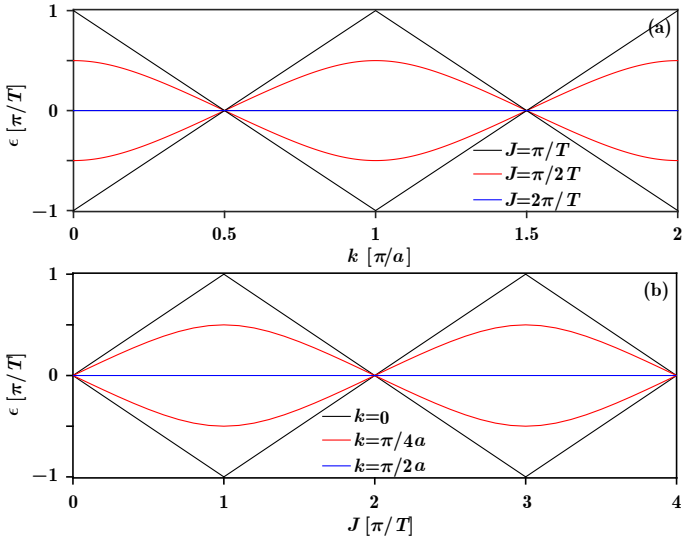

FIG. 3. (a) Quasi-energy as a function of k for different J values. (b) Quasi-energy as a function of J for different k values.

The situation changes qualitatively when the superlattice is truncated in the transverse direction. In this case one cannot introduce Bloch momentum anymore, so evolution dynamics is described by the system (1), where equations

for amplitudes in the edge sites A_1 and A_N are replaced by the equations $idA_1/dz = J_1(z)B_1$, $idA_N/dz = J_2(z)B_{N-1}$. One should stress that the properties of the system do not change qualitatively if superlattice is truncated on the site belonging to sublattice A on the left side, and on the site belonging to sublattice B on the right side. By introducing effective Hamiltonian for the finite longitudinally modulated superlattice, one can determine its quasi-energies that can be plotted as a function of the coupling strength J. In Fig. 4(a) we display corresponding dependence. One can see that this dependence inherits some features of $\epsilon(J)$ dependence of the infinite lattice [compare Figs. 4(a) and 3(b)]. Among them is the (partial) collapse of the quasi-energy band for specific values of the coupling constant $J = 2\pi m/T$. At the same time, there are two qualitative differences. First, within the interval $J \in [\pi/T,\ 3\pi/T]$ of coupling constants the isolated quasi-energies emerged (see red lines) that are associated with edge states. In fact, such edge states appear periodically in the intervals $[(4m+1)\pi/T,\ (4m+3)\pi/T]$, where m is an integer. The second difference is that the period of the $\epsilon(J)$ dependence is doubled in comparison with dependence in the infinite lattice. Qualitative modification of the quasi-energy spectrum indicates on the topological transition that occurs in finite modulated superlattice upon variation of coupling strength between waveguides. Interestingly, the collapse of quasi-energy band at $J = 2\pi/T$ indicating on the presence of dynamic localization in the system coexists with the fact of formation of edge states, so for this particular value of J two qualitative different localization mechanisms are simultaneously available.

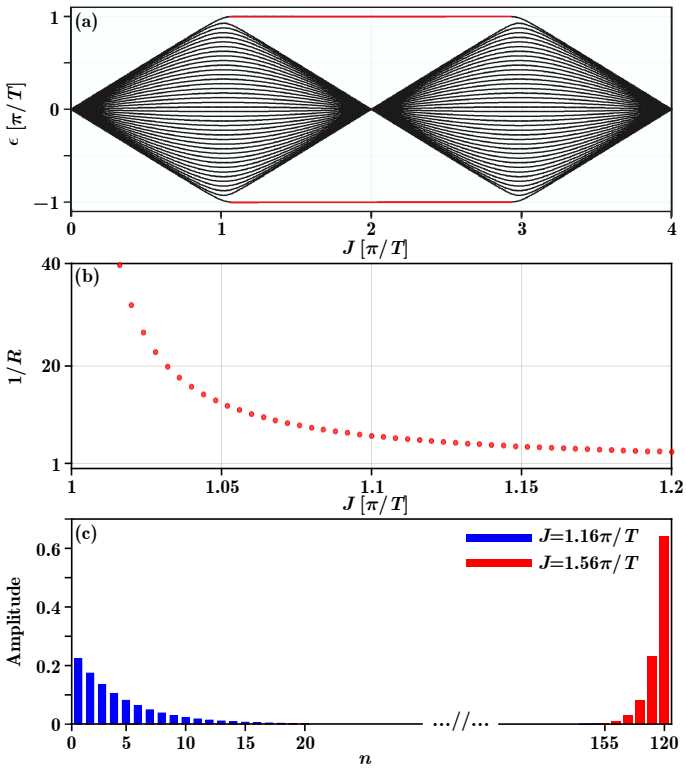

FIG. 4. (a) Dependence of quasi-energies on the coupling constant in the finite superlattice containing 200 sites in each sublattice. (b) Width of the edge state versus coupling constant. (c) Absolute value of the edge states corresponding to $J = 1.16\pi/T$ and $J = 1.56\pi/T$, respectively.

The width of emerging edge states strongly depends on the coupling constant. To illustrate this we introduce the participation ratio $R = \sum_n |q_n|^4/(\sum_n |q_n|^2)^2$, where $q_n = A_n, B_n$ stands for light amplitudes on sites of sublattices A and B. The width of the mode is inversely proportional to participation ratio. In Fig. 4(b), we show the width of the edge state versus coupling constant J. Localization increases with increase of coupling constant, so that already at $J > 1.1\pi/T$ the edge state occupies less than ten sites of the lattice. Maximal localization in nearly single surface channel occurs at $J = 2\pi/T$, and further increase of the coupling constant leads to gradual delocalization of the edge state. Examples of profiles of edge states (absolute value) with notably different localization degrees at $J = 1.16\pi/T$ and $J = 1.56\pi/T$ are shown in Fig. 4(c) .

III. TRANSPORT PROPERTIES

Topological transition that occurs in finite longitudinally modulated superlattice suggests the existence of novel propagation scenarios in this system. To study transport properties in such structures we simultaneously consider excitations of the internal and edge sites and use three representative values of the coupling constant. In the particular realization of the lattice, that we use to study propagation dynamics (see Fig. 5) two edge sites belong to different sublattices, i.e. the "bottom" site belongs to sublattice A, while the "top" site belongs to sublattice B. First, we consider the case $J = 0.5\pi/T$, where quasi-energy band has finite width, while edge states do not appear. In Fig. 5(a), we excite the internal waveguide and find that the beam diffracts during propagation. Similarly, the excitation of the edge waveguide shown in Fig. 5(b) is also accompanied by rapid diffraction without any signatures of localization. Second, we turn to the system with the coupling strength $J = 1.5\pi/T$. For this coupling constant according to Fig. 4(a), the width of the quasi-energy band is still finite, but edge states already emerge. Therefore, if an internal site is excited, discrete diffraction will be observed as shown in Fig. 5(c). In contrast, excitation of the edge site leads to the formation of well-localized edge state and only weak radiation can be detected, as shown in Fig. 5(d). The reason for small radiation is that we use excitation that does not match directly the shape of the edge state, hence delocalized bulk modes are excited too, but with small weights. Finally, we consider the case with $J = 2\pi/T$, where quasi-energy band collapses [Fig. 4(a)]. In this particular case dynamic localization occurs irrespectively of the location of the excited site. In Fig. 5(e), we show such a localization for excitations of sites number 10, 20, and 30. In addition, we also excite the edge waveguides in Fig. 5(f), where one can see that light beam does not experience expansion and remains confined in two near-surface sites. This is the regime where two distinct localization mechanisms coexist.

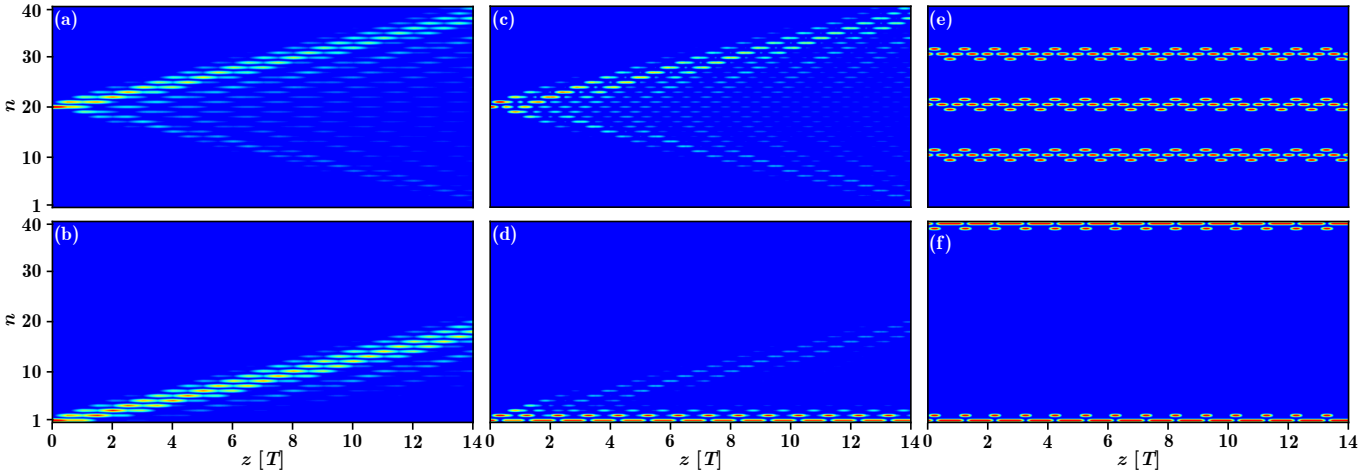

FIG. 5. Propagation dynamics in the finite superlattice when only one site in sublattice A is excited by the beam $\exp[-16\ln 2\,(x-x_A)^2]$, where x_A is the coordinate of the site in sublattice A. Left panels: internal site is excited. Right panels: edge site is excited. First column: $J = 0.5\pi/T$. Second column: $J = 1.5\pi/T$. Third column: $J = 2\pi/T$. Parameters: $a = 1$ and $T = 1$.

The propagation dynamics in this system is specific at $J = \pi/T$ and it deserves separate discussion. In the infinite lattice this coupling constant corresponds to linear dependence of quasi-energy on Bloch momentum k, i.e. the absence of diffraction (rectification regime). Finite superlattice inherits this property to some extent, i.e. localized excitations in finite lattice also do not diffract, but move with constant transverse velocity. Interestingly, despite the absence of diffraction, the excitation of edge states in this regime does not occur, since moving excitations just change their propagation direction when they hit edge sites. This is illustrated in Figs. 6(a) and 6(b), where we simultaneously excite two opposite edge waveguides. In this particular case we excited sites belonging to different sublattices, as before, but dynamics does not change qualitatively if sites from one sublattice are excited. Notice that in this interesting regime the transverse confinement occurs without any nonlinearity, and at the same time the propagation trajectory of the beam and its output position can be flexibly controlled that is advantageous for practical applications. To illustrate enhanced robustness of edge states introduced here we deliberately introduce considerable deformation at the surface of the lattice, by replacing the whole section of the edge waveguide between $z = T$ and $z = 2.5T$ with a straight section, as shown schematically in Fig. 6(c). The coupling constant for internal waveguides is selected as $J = 1.8\pi/T$, i.e. it corresponds to situation when edge states form at the surface. The corresponding propagation dynamics in this deformed structure is shown in Fig. 6(d). Despite considerable deformation of the structure the edge excitation passes the defect without noticable scattering into the bulk of the lattice. However, it should be mentioned that if surface defect is too long and extends over three or more periods of the structure, the

edge state may be destroyed and light will penetrate into the depth of the lattice. Finally, we design a structure that is composed of two parts with different coupling strengths between waveguides: in the first part of the lattice $J = \pi/T$ for closely spaced waveguides, while in the second part of the lattice $J = 1.5\pi/T$. Such variation in the coupling strength can be achieved by reduction of the transverse period at certain distance z, as shown in Fig. 6(e). Since in the first part of the lattice the coupling constant is selected such that no edge states can form, but diffractionless propagation is possible, the input beam will propagate from one edge of the lattice towards opposite edge. If it arrives to opposite edge in the point, where coupling constant changes and edge states become possible, the beam may excite the edge state and stay near the surface of the structure, as shown in Fig. 6(f). If, however, the beam hits the opposite edge before the point where coupling constant increases, it will be bounced back and enter into right half of the lattice in one of the internal waveguides. This will lead to fast diffraction of the beam without excitation of edge states. This setting can be considered as a kind of optical switch, where the presence of signal in the output edge channel depends on the position of the input excitation.

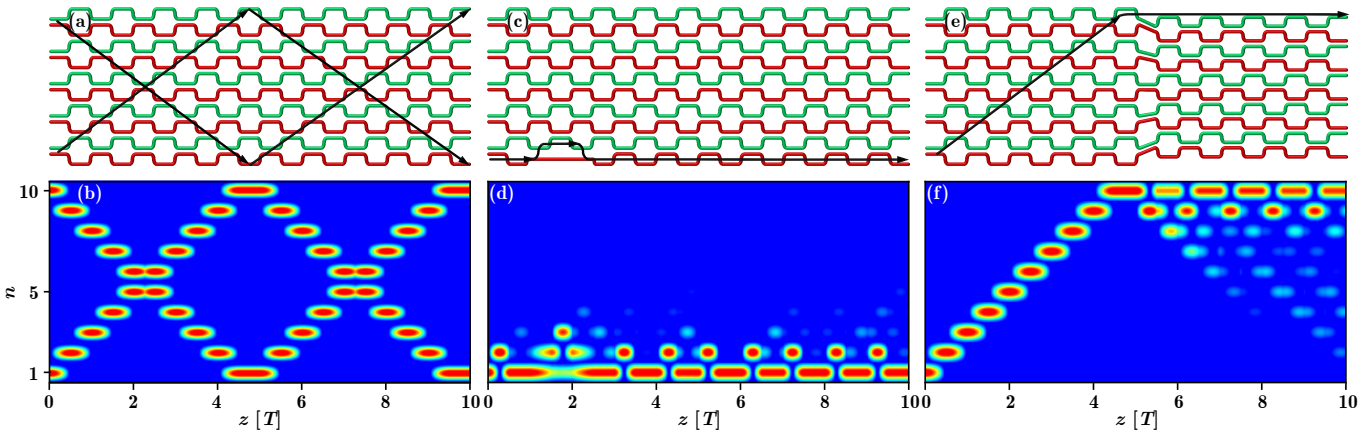

FIG. 6. (a) Schematic illustration of the waveguide array without defects or deformation. Black curve with arrows indicate the propagation direction for excitations of two opposite edge waveguides. (b) Propagation dynamics in the lattice without defects at $J = \pi/T$. (c) and (d) Same as (a) and (b), but for the system with a defect on the edge. For the internal waveguides, the coupling strength is $J = 1.8\pi/T$, while for the edge straight waveguide the coupling strength is $J = \pi/4T$ at $T < z \leq 1.5T$ and $2T < z \leq 2.5T$, and $J = \pi/15T$ at $1.5T < z \leq 2T$. (e) and (f) Same as (c) and (d), but for the lattice with global deformation that changes coupling constants after certain distance z. The coupling strength is $J = \pi/T$ at $0 \leq z < 5T$ and $J = 1.5\pi/T$ at $5T \leq z < 10T$.

IV. CONCLUSIONS

Summarizing, we investigated transport properties in the one-dimensional dynamical superlattices. We have shown that in finite modulated superlattices topological transition may occur that leads to appearance of edge states, whose degree of localization depends on the coupling constant between lattice sites. This localization mechanism may coexist with dynamic localization due to collapse of quasi-energy bands.

ACKNOWLEDGEMENT

This work was supported by China Postdoctoral Science Foundation (2016M600777, 2016M600776, 2016M590935), the National Natural Science Foundation of China (11474228, 61605154), and Qatar National Research Fund (NPRP 6-021-1-005, 8-028-1-001).

[1] T. Oka and H. Aoki, *Photovoltaic Hall effect in graphene*, Phys. Rev. B **79**, 081406 (2009).
[2] T. Kitagawa, E. Berg, M. Rudner, and E. Demler, *Topological characterization of periodically driven quantum systems*, Phys. Rev. B **82**, 235114 (2010).

[3] N. H. Lindner, G. Refael, and V. Galitski, *Floquet topological insulator in semiconductor quantum wells*, Nat. Phys. **7**, 490 (2011).

[4] M. S. Rudner, N. H. Lindner, E. Berg, and M. Levin, *Anomalous Edge States and the Bulk-Edge Correspondence for Periodically Driven Two-Dimensional Systems*, Phys. Rev. X **3**, 031005 (2013).

[5] A. Gómez-León and G. Platero, *Floquet-Bloch Theory and Topology in Periodically Driven Lattices*, Phys. Rev. Lett. **110**, 200403 (2013).

[6] N. Goldman and J. Dalibard, *Periodically Driven Quantum Systems: Effective Hamiltonians and Engineered Gauge Fields*, Phys. Rev. X **4**, 031027 (2014).

[7] J. K. Asboth and J. M. Edge, *Edge-state-enhanced transport in a two-dimensional quantum walk*, Phys. Rev. A **91**, 022324 (2015).

[8] T.-S. Xiong, J. Gong, and J.-H. An, *Towards large-Chern-number topological phases by periodic quenching*, Phys. Rev. B **93**, 184306 (2016).

[9] P. Titum, E. Berg, M. S. Rudner, G. Refael, and N. H. Lindner, *Anomalous Floquet-Anderson Insulator as a Nonadiabatic Quantized Charge Pump*, Phys. Rev. X **6**, 021013 (2016).

[10] Z. Yu and S. Fan, *Complete optical isolation created by indirect interband photonic transitions*, Nat. Photon. **3**, 91 (2009).

[11] K. Fang, Z. Yu, and S. Fan, *Realizing effective magnetic field for photons by controlling the phase of dynamic modulation*, Nat. Photon. **6**, 782 (2012).

[12] T. Kitagawa, M. A. Broome, A. Fedrizzi, M. S. Rudner, E. Berg, I. Kassal, A. Aspuru-Guzik, E. Demler, and A. G. White, *Observation of topologically protected bound states in photonic quantum walks*, Nat. Commun. **3**, 882 (2012).

[13] A. B. Khanikaev, S. H. Mousavi, W.-K. Tse, M. Kargarian, A. H. MacDonald, and G. Shvets, *Photonic topological insulators*, Nat. Mater. **12**, 233 (2012).

[14] G. Q. Liang and Y. D. Chong, *Optical Resonator Analog of a Two-Dimensional Topological Insulator*, Phys. Rev. Lett. **110**, 203904 (2013).

[15] M. C. Rechtsman, J. M. Zeuner, Y. Plotnik, Y. Lumer, D. Podolsky, F. Dreisow, S. Nolte, M. Segev, and A. Szameit, *Photonic Floquet topological insulators*, Nature **496**, 196 (2013).

[16] W.-J. Chen, S.-J. Jiang, X.-D. Chen, B. Zhu, L. Zhou, J.-W. Dong, and C. T. Chan, *Experimental realization of photonic topological insulator in a uniaxial metacrystal waveguide*, Nat. Commun. **5**, 5782 (2014).

[17] D. Leykam, M. C. Rechtsman, and Y. D. Chong, *Anomalous Topological Phases and Unpaired Dirac Cones in Photonic Floquet Topological Insulators*, Phys. Rev. Lett. **117**, 013902 (2016).

[18] D. Leykam and Y. D. Chong, *Edge Solitons in Nonlinear-Photonic Topological Insulators*, Phys. Rev. Lett. **117**, 143901 (2016).

[19] S. Weimann, M. Kremer, Y. Plotnik, Y. Lumer, S. Nolte, K. G. Makris, M. Segev, M. C. Rechtsman, and A. Szameit, *Topologically protected bound states in photonic parity-time-symmetric crystals*, Nat. Mater. **16**, 433 (2017).

[20] S. Longhi, *Quantum-optical analogies using photonic structures*, Laser Photon. Rev. **3**, 243 (2009).

[21] I. L. Garanovich, S. Longhi, A. A. Sukhorukov, and Y. S. Kivshar, *Light propagation and localization in modulated photonic lattices and waveguides*, Phys. Rep. **518**, 1 (2012).

[22] Y. Q. Zhang, Z. K. Wu, M. R. Belić, H. B. Zheng, Z. G. Wang, M. Xiao, and Y. P. Zhang, *Photonic Floquet topological insulators in atomic ensembles*, Laser Photon. Rev. **9**, 331 (2015).

[23] L. J. Maczewsky, J. M. Zeuner, S. Nolte, and A. Szameit, *Observation of photonic anomalous Floquet topological insulators*, Nat. Commun. **8**, 13756 (2017).

[24] M. A. Broome, A. Fedrizzi, B. P. Lanyon, I. Kassal, A. Aspuru-Guzik, and A. G. White, *Discrete Single-Photon Quantum Walks with Tunable Decoherence*, Phys. Rev. Lett. **104**, 153602 (2010).

[25] L. Sansoni, F. Sciarrino, G. Vallone, P. Mataloni, A. Crespi, R. Ramponi, and R. Osellame, *Two-Particle Bosonic-Fermionic Quantum Walk via Integrated Photonics*, Phys. Rev. Lett. **108**, 010502 (2012).

[26] J. K. Asbóth, B. Tarasinski, and P. Delplace, *Chiral symmetry and bulk-boundary correspondence in periodically driven one-dimensional systems*, Phys. Rev. B **90**, 125143 (2014).

[27] V. Dal Lago, M. Atala, and L. E. F. Foa Torres, *Floquet topological transitions in a driven one-dimensional topological insulator*, Phys. Rev. A **92**, 023624 (2015).

[28] S. Longhi, M. Marangoni, M. Lobino, R. Ramponi, P. Laporta, E. Cianci, and V. Foglietti, *Observation of Dynamic Localization in Periodically Curved Waveguide Arrays*, Phys. Rev. Lett. **96**, 243901 (2006).

[29] I. L. Garanovich, A. A. Sukhorukov, and Y. S. Kivshar, *Defect-Free Surface States in Modulated Photonic Lattices*, Phys. Rev. Lett. **100**, 203904 (2008).

[30] A. Szameit, I. L. Garanovich, M. Heinrich, A. A. Sukhorukov, F. Dreisow, T. Pertsch, S. Nolte, A. Tünnermann, and Y. S. Kivshar, *Observation of Defect-Free Surface Modes in Optical Waveguide Arrays*, Phys. Rev. Lett. **101**, 203902 (2008).

[31] S. Longhi and K. Staliunas, *Self-collimation and self-imaging effects in modulated waveguide arrays*, Opt. Commun. **281**, 4343 (2008).

[32] A. Szameit, Y. V. Kartashov, F. Dreisow, M. Heinrich, T. Pertsch, S. Nolte, A. Tünnermann, V. A. Vysloukh, F. Lederer, and L. Torner, *Inhibition of Light Tunneling in Waveguide Arrays*, Phys. Rev. Lett. **102**, 153901 (2009).

[33] S. Longhi, *Dynamic localization and transport in complex crystals*, Phys. Rev. B **80**, 235102 (2009).

[34] Y. V. Kartashov, A. Szameit, V. A. Vysloukh, and L. Torner, *Light tunneling inhibition and anisotropic diffraction engineering in two-dimensional waveguide arrays*, Opt. Lett. **34**, 2906 (2009).

[35] S. Longhi, *Rectification of light refraction in curved waveguide arrays*, Opt. Lett. **34**, 458 (2009).

[36] F. Dreisow, Y. V. Kartashov, M. Heinrich, V. A. Vysloukh, A. Tnnermann, S. Nolte, L. Torner, S. Longhi, and A. Szameit, *Spatial light rectification in an optical waveguide lattice*, EPL (Europhys. Lett.) **101**, 44002 (2013).

[37] Y. V. Kartashov, V. A. Vysloukh, V. V. Konotop, and L. Torner, *Diffraction control in $\mathcal{PT}$-symmetric photonic lattices: From beam rectification to dynamic localization*, Phys. Rev. A **93**, 013841 (2016).

[38] J. K. Asbóth, L. Oroszlány, and A. Pályi, *The Su-Schrieffer-Heeger (SSH) Model*, in *A Short Course on Topological Insulators: Band Structure and Edge States in One and Two Dimensions* (Springer, Cham, 2016) pp. 1–22.

[39] Y. Plotnik, M. C. Rechtsman, D. Song, M. Heinrich, J. M. Zeuner, S. Nolte, Y. Lumer, N. Malkova, J. Xu, A. Szameit, Z. Chen, and M. Segev, *Observation of unconventional edge states in 'photonic graphene'*, Nat. Mater. **13**, 57 (2014).

[40] R. A. Vicencio, C. Cantillano, L. Morales-Inostroza, B. Real, C. Mejía-Cortés, S. Weimann, A. Szameit, and M. I. Molina, *Observation of Localized States in Lieb Photonic Lattices*, Phys. Rev. Lett. **114**, 245503 (2015).

[41] S. Mukherjee, A. Spracklen, D. Choudhury, N. Goldman, P. Öhberg, E. Andersson, and R. R. Thomson, *Observation of a Localized Flat-Band State in a Photonic Lieb Lattice*, Phys. Rev. Lett. **114**, 245504 (2015).

[42] F. Diebel, D. Leykam, S. Kroesen, C. Denz, and A. S. Desyatnikov, *Conical Diffraction and Composite Lieb Bosons in Photonic Lattices*, Phys. Rev. Lett. **116**, 183902 (2016).

[43] A. Szameit, M. C. Rechtsman, O. Bahat-Treidel, and M. Segev, *$\mathcal{PT}$-symmetry in honeycomb photonic lattices*, Phys. Rev. A **84**, 021806 (2011).

[44] S. Weimann, L. Morales-Inostroza, B. Real, C. Cantillano, A. Szameit, and R. A. Vicencio, *Transport in Sawtooth photonic lattices*, Opt. Lett. **41**, 2414 (2016).

[45] J. H. Shirley, *Solution of the Schrödinger Equation with a Hamiltonian Periodic in Time*, Phys. Rev. **138**, B979 (1965).

[46] H. Sambe, *Steady States and Quasienergies of a Quantum-Mechanical System in an Oscillating Field*, Phys. Rev. A **7**, 2203 (1973).

[47] G. Della Valle and S. Longhi, *Spectral and transport properties of time-periodic $\mathcal{PT}$-symmetric tight-binding lattices*, Phys. Rev. A **87**, 022119 (2013).